

# Size effect of high contrast gratings in VCSELs

Christopher Chase, Ye Zhou, and Connie J. Chang-Hasnain\*

Department of Electrical Engineering and Computer Sciences, University of California, Berkeley, CA 94720, USA  
\*cch@eecs.berkeley.edu

**Abstract:** We report on the effects of shrinking the physical size of a high index contrast grating (HCG) on a vertical cavity surface-emitting laser (VCSEL). HCGs previously had been simulated assuming infinite periodicity. Here we probe through simulation and experiment the effect of reducing the HCG to only a few periods. We experimentally realize lasing VCSELs with as few as 4 periods of HCG. By shrinking the HCG to an extremely small size and integrating it on a wavelength tunable VCSEL, we are able to achieve a tunable VCSEL with a record fast mechanical tuning response of >27 MHz. This is a 5X improvement over the fastest previously reported wavelength tunable VCSELs.

©2009 Optical Society of America

OCIS codes: (250.7260) Vertical-cavity surface-emitting lasers; (140.3600) Tunable Laser

---

## References and Links

1. C. J. Chang-Hasnain, "Tunable VCSEL," *IEEE J. Sel. Top. Quantum Electron.* **6**(6), 978–987 (2000).
2. M. Lackner, M. Schwarzott, F. Winter, B. Kogel, S. Jatta, H. Halbritter, and P. Meissner, "CO and CO<sub>2</sub> spectroscopy using a 60 nm broadband tunable MEMS-VCSEL at 1.55 $\mu$ m," *Opt. Lett.* **31**(21), 3170–3172 (2006).
3. C. F. R. Mateus, M. C. Y. Huang, C. J. Chang-Hasnain, J. E. Foley, R. Beatty, P. Li, and B. T. Cunningham, "Ultra-sensitive immunoassay using VCSEL detection system," *Electron. Lett.* **40**(11), 649–651 (2004).
4. S. Decai, W. Fan, P. Kner, J. Boucart, T. Kageyama, Z. Dongxu, R. Pathak, R. F. Nabiev, and W. Yuen, "Long wavelength-tunable VCSELs with optimized MEMS bridge tuning structure," *IEEE Photon. Technol. Lett.* **16**(3), 714–716 (2004).
5. G. D. Cole, E. Behymer, T. C. Bond, and L. L. Goddard, "Short-wavelength MEMS-tunable VCSELs," *Opt. Express* **16**(20), 16093–16103 (2008).
6. C. F. R. Mateus, M. C. Y. Huang, D. Yunfei, A. R. Neureuther, and C. J. Chang-Hasnain, "Ultrabroadband mirror using low-index cladded subwavelength grating," *IEEE Photon. Technol. Lett.* **16**(2), 518–520 (2004).
7. Y. Ding, and R. Magnusson, "Resonant leaky-mode spectral-band engineering and device applications," *Opt. Express* **12**(23), 5661–5674 (2004).
8. M. C. Y. Huang, Y. Zhou, and C. J. Chang-Hasnain, "A surface-emitting laser incorporating a high-index-contrast subwavelength grating," *Nat. Photonics* **1**(2), 119–122 (2007).
9. S. Boutami, B. Benbakir, J. L. Leclercq, and P. Viktorovitch, "Compact and polarization controlled 1.55  $\mu$ m vertical-cavity surface-emitting laser using single-layer photonic crystal mirror," *Appl. Phys. Lett.* **91**(7), 071105 (2007).
10. M. C. Y. Huang, Y. Zhou, and C. J. Chang-Hasnain, "A nanoelectromechanical tunable laser," *Nat. Photonics* **2**(3), 180–184 (2008).
11. Y. Zhou, M. C. Y. Huang, and C. J. Chang-Hasnain, "Tunable VCSEL with ultra-thin high contrast grating for high-speed tuning," *Opt. Express* **16**(18), 14221–14226 (2008).
12. M. G. Moharam, and T. K. Gaylord, "Rigorous coupled-wave analysis of planar-grating diffraction," *J. Opt. Soc. Am.* **71**(7), 811–818 (1981).
13. V. Karagodsky, M. C. Huang, and C. J. Chang-Hasnain, "Analytical Solution and Design Guideline for Highly Reflective Subwavelength Gratings," in *Conference on Lasers and Electro-Optics/Quantum Electronics and Laser Science Conference and Photonic Applications Systems Technologies*, OSA Technical Digest (CD) (Optical Society of America, 2008), paper JTuA128.

---

## 1. Introduction

Wavelength tunable vertical-cavity surface-emitting lasers (VCSELs) have a wide variety of potential applications in areas such as telecommunications [1], spectroscopy [2], and biological/chemical sensing [3]. For these applications it is desirable to decrease wavelength-tuning time as much as possible to increase throughput. Given a required tuning range and maximum system voltage, MEMS-tunable VCSELs are limited in their tuning speed by the thickness of their movable mirror layer. In conventional MEMS tunable VCSEL designs, the

mirror is made up of a distributed Bragg reflector (DBR), from 3  $\mu\text{m}$  up to 10  $\mu\text{m}$  thick. This limits conventional designs to mirrors with maximum tuning responses of  $\sim 1$  MHz [4, 5].

In the last few years high contrast gratings (HCGs) [6, 7] have been demonstrated as a suitable mirror in a VCSEL structure [8, 9], replacing the conventional top DBR mirror. A HCG, a single layer grating structure of high index material surrounded by a low index material, can be less than 5% the thickness of the DBR it replaces. By integrating a transverse magnetic (TM)-HCG (245 nm thick, for a reflectivity band at 850 nm) into the movable mirror element in place of a DBR, a significant improvement in tuning response, to 3.3 MHz, has been realized due to the 10X reduction in mirror thickness [10]. Recently, an even thinner (145 nm) transverse electric (TE)-HCG was integrated, resulting in a tuning response as high as 4.5 MHz [11].

Previous analysis [6, 7] of HCGs has been performed assuming the infinite periodicity along the direction of periodicity and infinitely long grating bars, but in practice they are finite. The reflectivity of a HCG does not have an obvious limitation based on the lateral area. Here we probe the limits of the lateral area required to provide enough reflectivity for a VCSEL to lase through simulation and experiment. By decreasing the area of the HCG to the smallest possible lateral area, we can further increase the resonance frequency of the mechanical structure because of the reduction in the mass of the mirror. This allows us to fabricate structures with resonance frequencies much higher than those in previous work.

## 2. VCSEL design and characteristics

The devices used in the simulations and experiment are of similar design to previous nano-electromechanical optoelectronic (NEMO) tunable VCSEL designs [10, 11]. A schematic of the completed tunable VCSEL structure is shown in Fig. 1. The structure is comprised of (from the substrate side) 34 pairs of  $n$ -DBR, an active region with 3 quantum wells designed to emit at 850 nm, an oxide aperture for current confinement, and a top mirror consisting of 2 or 4 pairs of  $p$ -DBR, an air gap, and finally a 145 nm thick  $n$ -TE-HCG layer.

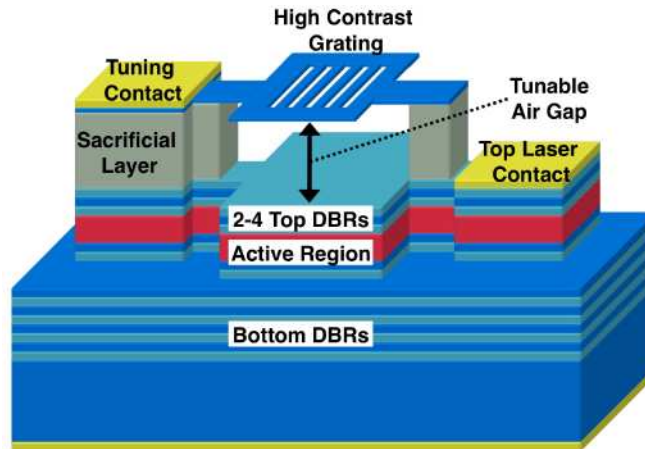


Fig. 1. Schematic of a NEMO tunable VCSEL with a suspended TE-HCG in place of a typical top DBR.

The TE-HCG used in this study has a period of 640 nm, semiconductor duty cycle of  $\sim 38\%$ , HCG thickness of 145 nm, and an air gap of  $\sim 900$  nm under no tuning bias. The HCG is made up of  $\text{Al}_{0.6}\text{Ga}_{0.4}\text{As}$  surrounded by air as the low index material. Current is injected through top laser contact to the  $p$ -DBR, which is present in the design only to provide current injection and protect the active region, to a backside contact on the bottom of the substrate. The HCG is fixed to supports by beams made up of the HCG material and can be electrostatically actuated by applying a reverse-bias voltage between the top tuning contact

and top laser contact. This actuation changes the size of the air gap and cavity length, shifting the output wavelength of the device.

After epitaxial growth, the devices are fabricated by first depositing the tuning contact followed by a wet etch through to the bottom DBRs to form mesas. Next, selective thermal oxidation is used to form an oxide aperture for current confinement. Afterwards, a selective etch is performed to expose the  $p$ -DBR, and metal is evaporated on the exposed  $p$ -DBR to form the top laser contact. Finally e-beam lithography is used to pattern the HCG. The HCG pattern is transferred via dry etch and then released from the rest of the structure using a selective etch. This is followed by critical point drying to prevent pull-in of the HCG during the drying process.

The VCSEL devices with integrated TE-HCG show excellent optical characteristics. Devices have thresholds well below 1 mA and slope efficiencies greater than 0.5 W/A, which are similar to conventional designs based on a top DBR as a mirror. The devices presented here lase with only a single transverse mode. As the HCG mirror is designed to be highly reflective only for one orthogonal polarization, HCG VCSELs also lase in only one orthogonal polarization mode [11]. In the case of the TE-HCG, the electric field of the lasing mode is oriented parallel to the grating bars.

A light-current-voltage characteristic of a TE-HCG VCSEL is shown in Fig. 2(a). The differential resistance of these VCSELs is relatively high because doping in the  $p$ -layers of the top  $p$ -DBRs has not been optimized. Figure 2(b) shows the spectrum of a different tunable TE-HCG under various reverse bias voltages between the tuning contact and laser contact and at a constant laser drive current of 3.5 mA. A continuous tuning range of ~6 nm is obtained with the TE-HCG VCSEL with single mode operation over nearly the entire range. This tuning range is the widest reported with a TE-HCG. This expanded tuning range is obtained using only 2 pairs of  $p$ -DBR instead of 4 pairs. With more device structure optimization, this range should be expandable to greater than 15 nm as been shown with the TM-HCG VCSEL [10].

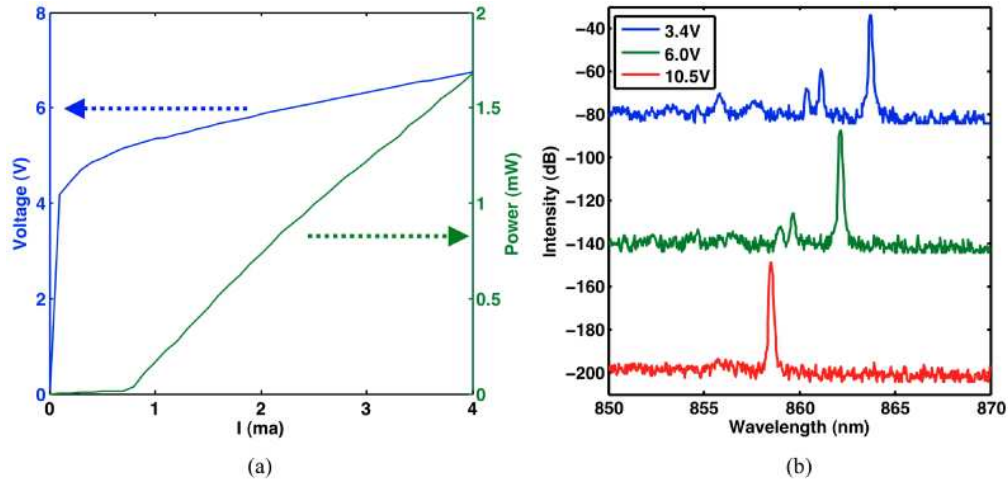


Fig. 2. (a) Light-current-voltage characteristic of a TE-HCG tunable VCSEL under continuous wave, room temperature operation. (b) Spectrum of another TE-HCG tunable VCSEL at constant bias current of 3.5 mA with the tuning contact under various reverse bias voltages (spectra offset by 60 dB).

### 3. Results

#### 3.1 Simulation results

HCG simulation and design are typically performed using the Rigorous Coupled Wave Analysis (RCWA) method [12]. This method assumes infinite periodicity, so the effect of reducing the grating to just a few periods is not obvious. Analytic treatment of the HCG

structure [13] shows that there are no propagating waves in the plane of the HCG, so intuitively the size of the HCG should not significantly effect the overall reflectivity of the grating, as there is no dependence of a given grating period on the number of periods to its sides.

To simulate the case of TE-HCGs with a finite number of periods, the reflectivity of a HCG was calculated using a finite-difference time-domain (FDTD) simulation (using the commercial software Lumerical FDTD Solutions). The simulation was performed varying two parameters: the grating size (number of periods) and the size of the oxide aperture. The reflectivity was calculated by launching a Gaussian beam with waist the size of the aperture through the entire top mirror structure, including 4 pairs of DBR, from the aperture and measuring the reflected power. The HCG dimensions used in the simulation were the TE-HCG dimensions described previously, and the wavelength of the Gaussian beam was 850 nm. From this reflectivity, mirror loss could be calculated for each case. The results are shown in Fig. 3. As the HCG is shrunk, the mirror loss is not significantly affected until the HCG becomes approximately the same size as the aperture itself. As the size is further decreased to less than the size of the aperture, the mirror loss increases significantly, since the high reflectivity HCG region no longer covers the whole beam area. This result indicates that in fact there is little effect on the reflectivity of the HCG on the number of periods of the HCG.

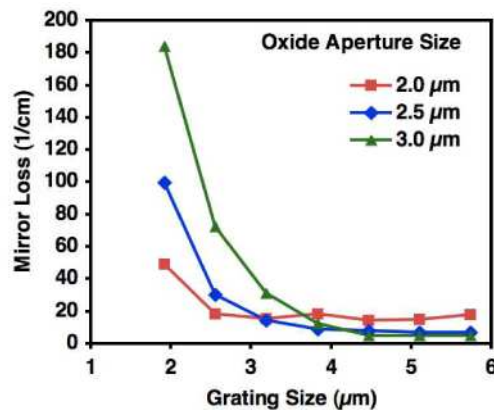


Fig. 3. Mirror loss of the TE-HCG structure as a function of mirror loss and grating size. The mirror loss of the device is constant until the HCG is slightly larger than the aperture size, indicating the reflectivity of the HCG is not significantly impacted by the number of periods in the structure.

### 3.2 Experimental results

To experimentally probe the effect of size of the TE-HCG on VCSEL performance, a series of TE-HCG tunable VCSELs were fabricated with square HCGs of sizes from 12 μm (18 periods) down to 2.3 μm (3 periods). The VCSELs in this study were fabricated on the same wafer at the same time to ensure uniformity. VCSELs were found to lase with just 4 period HCGs (2.9 μm × 3 μm × 145 nm). Scanning electron microscopy (SEM) images of the smallest working HCGs are shown in Fig. 4.

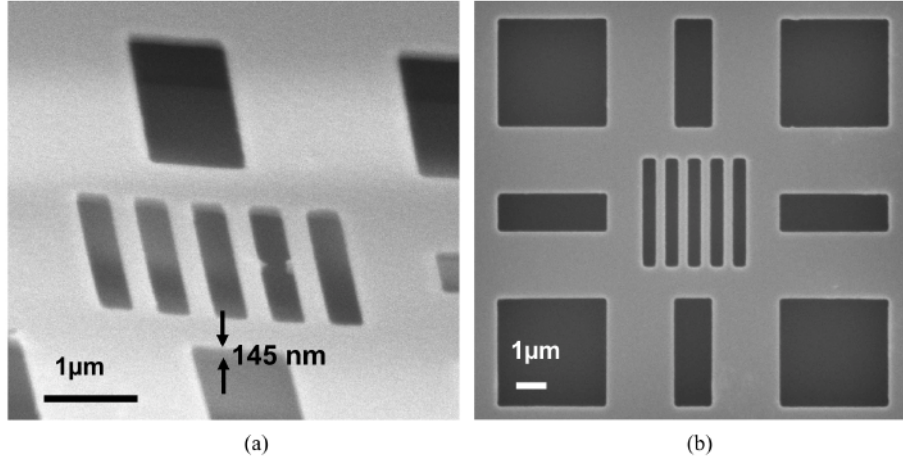


Fig. 4. SEM images of a  $2.9 \mu\text{m} \times 3 \mu\text{m} \times 145 \text{ nm}$  HCG, the smallest lasing HCG VCSEL (a) tilted view showing the 145 nm thickness of the TE-HCG (b) top view.

Light-current characteristics of the VCSELs with various sizes of TE-HCG are shown in Fig. 5. The devices have approximately the same size oxide aperture, estimated to be  $\sim 3 \mu\text{m}$ , and are otherwise identical except for the HCG size. It should be mentioned that the oxidation process was performed a  $100 \mu\text{m}$  size mesa and hence there is an inherent inaccuracy of  $\sim 1 \mu\text{m}$  between the HCG and oxide aperture. The VCSELs show similar characteristics until the HCG has less than 7 periods ( $4.8 \mu\text{m}$ ). When the HCG has fewer periods than 7, its threshold increases as period is further reduced. No devices with 3 periods lased experimentally. This trend matches well with the simulation, which shows that mirror loss and correspondingly laser threshold is constant until the HCG is only slightly larger than the aperture. These devices have an oxide aperture size of  $3 \pm 1 \mu\text{m}$ , so we observe a similar trend experimentally. This shows that in fact, the number of HCG periods does not have a significant effect on the overall reflectivity. Only the physical overlap of the mirror itself with the aperture is significant.

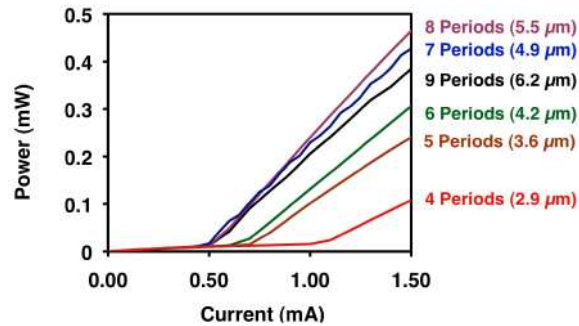


Fig. 5. Light-current characteristics of TE-HCG VCSELs with different size HCGs. Device characteristics are nearly unchanged until the HCG has less than 7 periods ( $4.8 \mu\text{m}$ ).

The mechanical frequency response of the HCG was measured by biasing the VCSEL at a constant current through the laser contact and applying between the tuning contact and laser contact a DC voltage with a sinusoidal AC modulating voltage, actuating the mirror. The modulating voltage causes the spectrum of the device to broaden in an optical spectrum analyzer (OSA) as the laser is changing wavelength many times over the OSA's slow sampling time ( $\sim 1 \text{ s/nm}$  with  $\sim 500$  sampling points per nm).

The spectrum of a device with a  $3.6 \mu\text{m}$  HCG with various AC modulation frequencies on the mechanical tuning contact is shown in Fig. 6(a). The device is driven at a  $1.4 \text{ mA}$  laser bias current with a  $22 \text{ V}$  DC bias and a  $10 \text{ V}$  peak-to-peak AC signal between the laser

contact and tuning contact to provide mechanical actuation. This device required higher tuning voltages than the device in Fig. 2, because its mechanical actuators were designed to be several times stiffer, requiring higher actuation voltages. The tuning range of the device in Fig. 6 is limited to  $< 1$  nm because a maximum voltage of  $\sim 40$  V can be applied between the tuning contact and laser contact before the blocking junction between the two contacts breaks down. The full tuning range could be achieved at this tuning speed by modifying the structure so that more electrostatic force can be applied; for example, by using aluminum oxide between the tuning and laser contact, or optimizing the air gap to get the best tradeoff between electrostatic force and breakdown voltage. Figure 6 (b) shows the relative optical tuning response from the mechanical tuning at various input frequencies. The response has two peaks due to two relatively closely spaced mechanical resonances. Our measurement setup is limited to 30 MHz. This ultra small HCG shows optical response to AC tuning signals up to a  $-3$  dB point of  $\sim 27$  MHz, 5X higher than previously reported HCG tunable VCSELs [11].

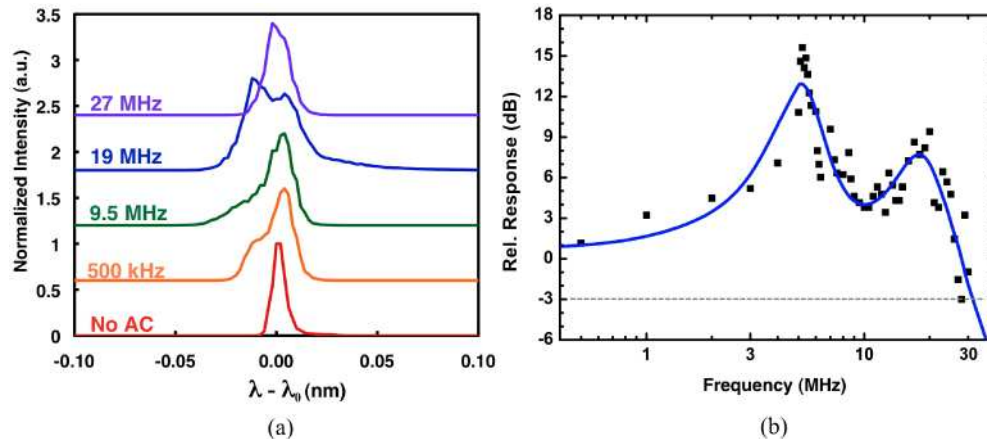


Fig. 6. (a) Spectrum of a tunable VCSEL at constant bias of 1.4 mA with a mechanical tuning signal between the tuning contact and laser contact of a DC voltage plus an AC voltage at various frequencies. (b) Relative optical wavelength change of the VCSEL as a function of input frequency to the tuning contact. The  $-3$ dB point in optical response occurs around 27 MHz.

#### 4. Conclusion

The effects of the size of a HCG are studied when incorporated on a tunable VCSEL through simulation and experiment. HCGs with as few as 4 periods ( $2.9 \mu\text{m} \times 3 \mu\text{m} \times 145 \text{ nm}$ ) are shown to provide sufficient reflectivity for a VCSEL to lase. VCSEL characteristics are shown to be nearly constant regardless of the size of the HCG, until the HCG is approximately the same size as the VCSEL aperture. With these compact HCGs, mechanical tuning response is seen up to a  $-3$  dB point of  $\sim 27$  MHz, 5X faster than previous reports. This increase of tuning speed may enable further applications of tunable VCSELs and other wavelength-tunable optoelectronic devices such as optical filters, sensors, and detectors.

#### Acknowledgements

The authors would like to acknowledge support from the National Science Foundation through CIAN NSF ERC under grant #EEC-0812072 and a National Science Foundation Graduate Research Fellowship. We also thank LandMark Optoelectronics Corporation for their growth of the epitaxial wafer and Berkeley Microfabrication Laboratory for their fabrication support.